Correlating Carbon Dioxide Capture and Chemical Changes in Pyrolyzed Polyethyleneimine-C_{60}

Enrico Andreoli[†,‡,*] *and Andrew R. Barron*[†,‡,§]

[†] Energy Safety Research Institute, Swansea University, Bay Campus, Swansea SA1 8QQ, UK.

[‡] Department of Chemistry, Rice University, Houston, TX 77005, USA.

[§] Department of Materials Science and Nanoengineering, Rice University, Houston, TX 77005, USA.

Nitrogen functionalities play a crucial role in determining the sorption capacity and selectivity of organic-based CO_2 solid sorbents. Two main types of solid sorbents are (1) amine-rich compounds used for their distinctive reactivity of amino groups with CO_2, and (2) N-doped carbons where CO_2-philic nitrogens impart chemoselectivity to otherwise pure carbon physisorbents. It is of interest to correlate the CO_2 sorption performance of these materials to the chemical changes involved in going from amine-rich polymers to N-doped carbons. To this end, we pyrolyzed amine-rich polyethyleneimine-C_{60} (PEI-C_{60}) to N-doped carbons and focused our investigation on how chemical changes and CO_2 capture correlate. In particular, we found that upon thermal treatment in inert atmosphere, PEI-C_{60} undergoes an inversion in CO_2 sorption behavior. PEI-C_{60}, which better absorbs CO_2 at high temperature (0.13 g/g at 90 °C), is converted into pyrolyzed materials with improved CO_2 capture performance at low temperature (0.12 g/g at 25 °C). XPS, FTIR, and Raman characterizations reveal a progressive conversion of

PEI-C_{60} to disordered graphitic carbon including pyrrolic and pyridinic aromatic nitrogens, where the transition from one material to the other goes through a drastic drop of CO_2 capture performance due to the breakdown of the carbon backbone of PEI.

1. INTRODUCTION

The Earth's climate has witnessed significant anomalies in 2014, the warmest year on record.[1] CO_2 emissions from human activities are among the major causes of global warming.[2] The social cost of CO_2 – i.e., the economic damage in dollars per ton of CO_2 on crops, human health and productivity, and the environment, for example[3] – is also under close scrutiny. In a recent estimate, it has been evaluated that this cost is six times higher than the value currently used to guide and establish new policies against climate change: $220/ton instead of the present $37/ton.[4] On the one hand, this can make existing and emerging CO_2 curbing technology cost-effective, but, on the other hand, it calls for an even greater effort in developing improved CO_2 capture materials and technologies. To that end, much research work has appeared in the literature in the last five years on a variety of solid state CO_2 absorbents based on different chemistries like amine-, carbon-, graphite/graphene-, zeolite-, MOF-, silica-, polymer-, clay-, alkali metal carbonate-, immobilized ionic liquid-, and CaO-based absorbents, to name some.[5-6] In particular, our research groups has focused its attention on preparing and characterizing the properties and performance of polyethyleneimine-modified nanocarbons (PEI-NCs).[7-11]

Among different PEI-NCs,[8] fullerene-C_{60} cross-linked polyethyleneimine (PEI-C_{60}) stands out in terms of ease of preparation and CO_2 capture performance. PEI-C_{60} has extremely high selectivity which makes it an ideal material for capturing CO_2 from flue gases and for purifying natural gas.[9] It also has a CO_2 capture capacity of 0.14 g/g at 90 °C at just 0.1 bar, making it one

of the highest performing materials is such operating conditions.[9] However, kinetic studies show that the rate of absorption of CO_2 in PEI-C_{60} is slow especially at room temperature because of gas diffusion limitations.[10] In one approach, we doubled the rate of CO_2 absorption by increasing the macroporosity of the materials through spray-drying and cryo-milling.[11] Following an alternative approach, here we present the results based on the thermal treatment of PEI-C_{60} in inert atmosphere. The rationale behind this approach is that thermally treating amine-rich polymers like PEI-C_{60} can induce significant chemical changes that might enhance the CO_2 capture performance of the resulting materials. Our goal is then to identify the chemical changes involved in the pyrolysis of PEI-C_{60} and correlated them to the CO_2 capture performance of the resulting materials.

Thermally treating materials in the absence of oxygen is a widely used procedure referred as to pyrolysis. Pyrolysis has been applied toward multiple purposes at industrial level for quite a long time,[12] but fresh interest has been recently driven up by the impelling energy and climate worldwide challenges focused in particular on the production of low-carbon footprint fuels. A number of recent reviews addressing the specific use of pyrolysis demonstrates this, especially in the fields of the conversion of biomass to fuel-bio-oil or catalytically to hydrocarbons compatible with the existing energy infrastructure,[13] the thermal breakdown and liquefaction of coal to fuels,[14] and the formation of hydrogen from the thermolysis of biomass.[15]

Pyrolysis has also been used in the preparation of solid-state materials. N-doped graphene has been obtained from the pyrolysis of graphene oxide and urea, the resulting materials have excellent catalytic activity toward the oxygen reduction reaction critical in the commercialization of fuel cells.[16-17] N-doped porous carbon for supercapacitor applications has also been prepared using pyrolysis.[18] Highly luminescent carbon nanodots,[19] ZnO nanorods for H_2S sensors,[20]

Ag/TiO_2 nanocomposites for the catalytic production of H_2 and reduction of CO_2,[21] and Cu_2ZnSnS_4 thin films for solar cell fabrication[22] are some examples of the versatility and utility of the different forms of pyrolysis. In the present case, we focused on applying pyrolysis to transform PEI-C_{60} in N-doped carbon materials and critically compare their CO_2 sorption performance.

2. EXPERIMENTAL

2.1 SAMPLES PREPARATION. All materials were used as received. Fullerene C_{60} (99.5%) was supplied by Alpha Aesar, polyethyleneimine branched (PEI, Mw 25 kDa), chloroform (+99.8%), toluene (99.9%) by Sigma Aldrich, and triethylamine (99%) by Acros. Ar and CO_2 high purity gases were all supplied by Matheson TRIGAS. 1.00-1.20 g of PEI dissolved in 35 ml of chloroform were added to a solution of 0.12 g of C_{60} in 150 ml toluene with 6 ml triethylamine. A dark-brown precipitate made of PEI-C_{60} was formed and then filtered on a PTFE membrane 0.45 μm pore size. Excess chloroform was used to wash the precipitate which was resuspended in 50 ml chloroform and filtered again as before. The precipitate was dried and collected as a clustery/rubbery brown solid. The thermal treatment in inert atmosphere of PEI-C_{60} was performed with a TA Instruments SDT Q600 TGA/DSC. 5-15 mg of sample was loaded in an alumina pan and heated up to a set pyrolysis temperature at a rate of 10 °C/min while flowing Ar at 50 ml/min. A final temperature of 100, 200, 300, 400, 500, 600, 700, 800, 900, and 1000 °C was held for 15 min. The pyrolyzed samples were allowed to cool down and transferred to the characterization equipment under Ar.

2.2 SAMPLES CHARACTERIZATION. The CO_2 capture performance of as prepared and thermolyzed PEI-C_{60} was characterized using a TA Instruments SDT Q600 TGA/DSC. PEI-C_{60}

was loaded in an alumina pan and thermally treated; after treatment, the resulting material was immediately characterized for isothermal CO_2 sorption. The CO_2 capture capacities are given in g CO_2 per g sorbent materials (g/g). X-ray photoelectron spectroscopy (XPS) was performed using a Physical Electronics PHI Quantera SXM equipped with an Al X-ray monochromatic source (Kα 1486.6 eV) set at a 200 mm beam diameter and a 45° incident angle. Binding energy referred to adventitious carbon (C1s 284.8 eV). The high-resolution spectra were fitted with peaks using mixed Gaussian-Lorentzian curves after subtraction of a Shirley-type background. For comparison purposes, the full width at half maximum (FWHM) of the peaks of pyrolyzed sample was fixed at 1.4 eV. Raman spectroscopy was performed using a Renishaw inVia Raman microscope equipped with a 633 nm laser. Attenuated total reflectance Fourier transform infrared spectroscopy (ATR-FTIR) was performed with a Nicolet Nexus 670 FT-IR with a diamond window.

3. RESULTS AND DISCUSSION

PEI-C_{60} was thermally treated in Ar at various temperatures and the CO_2 uptake evaluated after each treatment, as presented in Figure 1. The treatment temperatures were 100, 200, 400, 600, 800, and 1000 °C. The weight loss and heat flow profiles recorded during pyrolysis are given in Figure S1 of the Supporting Information. The CO_2 uptake was carried out at three different temperatures 25, 45, and 90 °C. At 25 °C, it is evident that the CO_2 capture capacity of PEI-C_{60} increases with increasing temperature of treatment (Figure 1a). In particular, the capture capacity goes from about 0.005 to 0.12 g/g for PEI-C_{60} treated at 100 and 1000 °C, respectively. At 45 °C, the CO_2 absorption capacity of the sample treated at 100 °C is higher than that treated at 200 °C (Figure 1b), which capacity is roughly unchanged compared to that measured at 25 °C (Figures 1a and 1b).

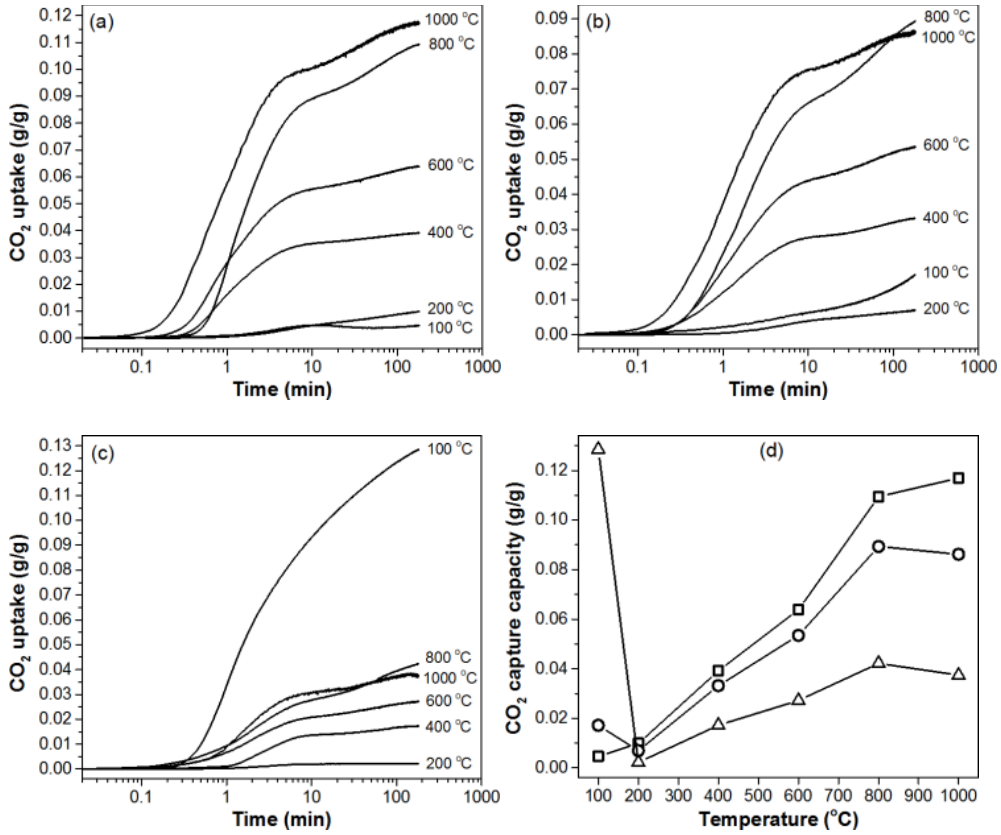

Figure 1. CO_2 sorption performance of PEI-C_{60} after thermal treatment/pyrolysis. CO_2 uptake at 25°C (a), 45°C (b), and 90°C (c) in single component CO_2 at atmospheric pressure. PEI-C_{60} was treated in Ar at the temperatures shown beside each curve in plots (a), (b), and (c). In plot (d), the dependence of the CO_2 capture capacity of PEI-C_{60} from the treatment temperature for CO_2 sorptions performed at 25°C (□), 45°C (○), and 90°C (△).

Interestingly, the CO_2 sorption capacity of the sample treated at 800 °C surpasses that of PEI-C_{60} pyrolyzed at 1000 °C, and overall the capacities of all samples are lower than those recorded at 25 °C. At 90 °C, the absorption capacity of PEI-C_{60} heated at 100 °C improves drastically climbing well above that of all other materials treated at higher temperatures. PEI-C_{60} performs particularly well at higher sorption temperatures because of the increased diffusion of CO_2 in the bulk of the material.[9-11] A comparison of CO_2 capture capacities in function of the treatment

temperature is given in Figure 1d. A peculiar feature of this plot is the presence of an inversion point at 200 °C where the CO_2 absorption capacity is lowest and does not change significantly with the temperature of absorption. For treatment temperatures below 200 °C, the CO_2 absorption capacity of PEI-C_{60} excels at higher temperature. For example, the capacity of the sample treated at 100 °C goes from 0.005 to 0.13 g/g at temperature of absorption of 25 and 90 °C, respectively. This trend is reversed at treatment temperature above 200 °C. In particular, the CO_2 absorption capacity of the sample pyrolyzed at 1000 °C is higher at low temperature reaching its maximum capacity of about 0.12 g/g at 25 °C. The CO_2 capture capacity of the resulting N-doped graphitic materials (up to 2.72 mmol/g) is below that of other previously developed N-doped carbon-based materials, e.g., 5.14 mmol/g for highly porous N-doped activated carbon monoliths at ambient pressure and temperature.[23] However, we want to emphasize that the focus of the present work is to identify the relationship existing between CO_2 sorption and chemical changes of amine-rich polymer composites upon thermal treatment in inert atmosphere.

Furthermore, in terms of CO_2 sorption kinetics, a comparison of the CO_2 sorption curves of pyrolyzed PEI-C_{60} (Figure 1) indicates that pyrolyzing at higher temperature affords materials with faster sorption kinetics because of the increasing contribution of physical sorption over chemical sorption in samples pyrolyzed at higher temperature. In fact, the sorption capacity of physical sorbents is known to increase with decreasing sorption temperature, as observed in the present case for all pyrolyzed samples. On the other hand, for the as prepared PEI-C_{60} chemical sorption is still effective at high temperature given the reactivity of CO_2 with amines. PEI-C_{60} is the only sample with increased CO_2 capacity and faster kinetics at high temperature opposite to what observed for the pyrolyzed samples.

The effect of thermal treatment on the weight and composition of PEI-C_{60} is presented in Figure 2. PEI-C_{60} loses about 30% of its original weight upon heating at 100 °C (Figure 2a); this is mainly due to the removal of adsorbed gases and moisture present in the material.[9] In this regard, it is important to notice that thermal treatment at 90-100 °C does not alter the CO_2 absorption performance of PEI-C_{60}.[9] Interestingly, the weight loss is essentially the same when the material is treated at 200 °C (Figure 2a), indicating that the bulk of the material can tolerate quite high temperatures for a polymer. However, although the mass of PEI-C_{60} remains essentially unchanged in going from 100 to 200 °C, the CO_2 capture capacity drops dramatically, as shown in the absorption data presented in Figure 1d. An explanation for this drastic deterioration of CO_2 capture performance without significant mass loss in the bulk of the material might be related to the breaking of the chemical bonds of PEI-C_{60} and loss of volatiles only from the surface of the material.

In support to this hypothesis are the results presented in Figure 2b, the data indicate that the nitrogen concentration present on the surface of the material (measured in the top 5-10 nm layer by XPS) drops from about 30 to 25% in going from 100 to 200 °C thermal treatment, respectively. Furthermore, XPS and IR results indicate that at 200 °C PEI-C_{60} undergoes C-N molecular backbone breakdown with correspondent increase in amine functionalities (*vide infra*). In this case, a greater number of free amine groups causes the material to become sticky and viscous limiting the diffusion and uptake of CO_2. Thus, it appears that the thermal alteration of the molecular backbone of PEI is responsible for the drastic drop of CO_2 absorption performance after treatment at 200 °C. A further increase in the temperature of pyrolysis causes a progressive weight loss (Figure 2a) with the weight dropping to residual values of as low as 20% after pyrolysis at 1000 °C. Correspondingly, the nitrogen concentration present on the material falls

from 30 to 5%. In this case, these large weight losses indicate that the bulk of PEI-C_{60} has been fully pyrolyzed.

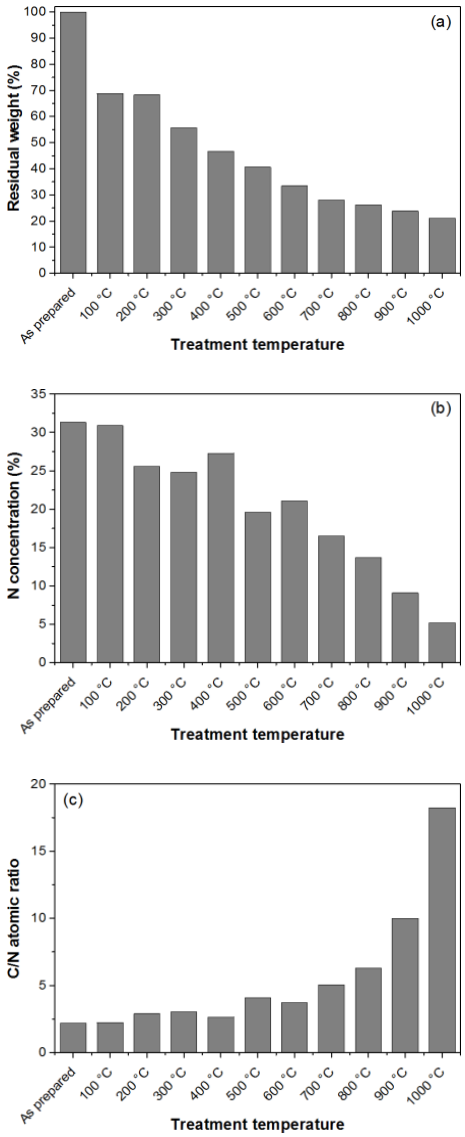

Figure 2. Weight and composition change of PEI-C_{60} upon thermal treatment. Percent weight of PEI-C_{60} remaining after treatment/pyrolysis measured using TGA (a). Atomic nitrogen concentration (b) and atomic carbon/nitrogen ratio (c) present on the surface of PEI-C_{60} after treatment/pyrolysis measured using XPS.

Particularly informative is also the carbon/nitrogen atomic ratio of PEI-C_{60} and how it varies upon thermal treatment/pyrolysis (Figure 2c). The surface C/N ratio of as prepared PEI-C_{60} is 2.2 in agreement with the chemical composition of PEI, $(C_2H_5N)_n$, with 10% extra carbon atoms due to C_{60}. This ratio changes only slightly for treatment temperatures of up to 400 °C with C/N values remaining within 3. Instead, for temperatures above 400 °C there is a progressive loss of nitrogen reaching a C/N ratio of 18 at 1000 °C. It is found that this change of C/N ratio is due to the formation of carbazole- and quinoline-like moieties upon thermolysis (*vide infra*).

PEI-C_{60} samples have been characterized using XPS to obtain information on the chemical changes induced upon thermal treatment. The C1s and N1s high resolution spectra of PEI-C_{60} before and after thermal treatment are presented in Figure 3. From a quick look at the signals, it is evident that the composition of the samples changes drastically upon heating in inert atmosphere. In the case of as prepared PEI-C_{60} two peaks are found for both C1s and N1s, whereas multiple peaks start appearing already after treatment at 200 °C. More peaks are recorded for higher treatment temperatures. The evolution of the peaks with corresponding assignments is discussed below.

The fitting results of the XPS C1s spectra of PEI-C_{60} are collected in Table 1. For comparison purposes, all spectra were deconvoluted with peaks of fixed FWHM at 1.4 eV. The fitting peaks are separated and organized in groups each belonging to a specific assignment group. The as prepared PEI-C_{60} has two peaks associated to the aliphatic (C-C) and amine (C-N)

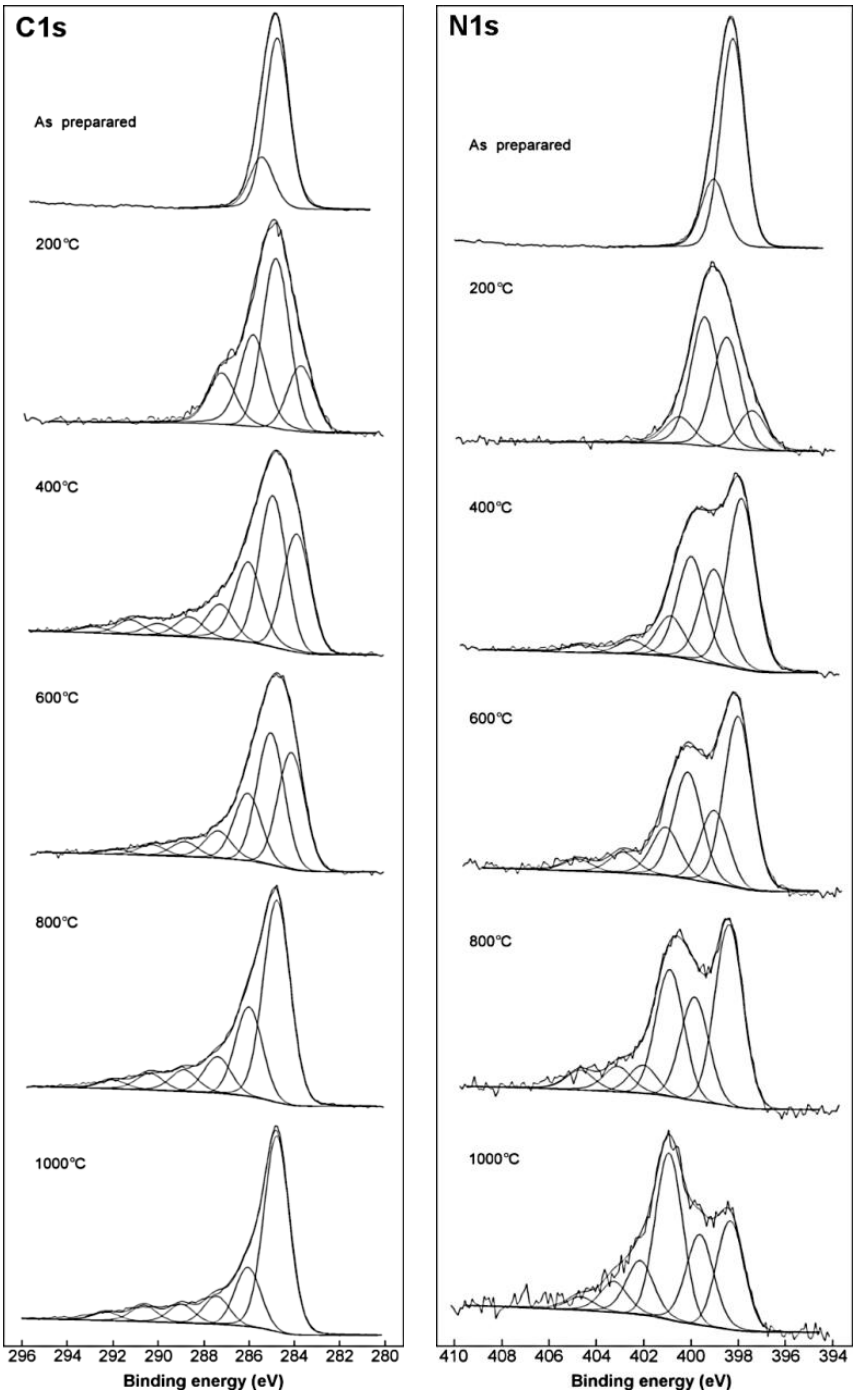

Figure 3. XPS C1s (left) and N1s (right) high resolution spectra of as prepared and thermally treated PEI-C_{60}.

Table 1. XPS C1s peak positions (eV), relative intensities (%, reported in parenthesis), and assignments for as prepared and thermally treated PEI-C_{60}.

PEI-C_{60} Treatment T	Peaks and Assignments							
	Aromatic carbon	Aliphatic carbon / Graphite-like carbon	Amine / Hydroxyl / N-doped graphite	Amide / N-doped graphite	Aldehydes / Ketones	Carboxylate group	Carbonates / π→π* shake-up satellites	
As prepared	-	284.7 (76.0)	285.5 (24.0)	-	-	-	-	-
200 °C	283.8 (29.0)	284.4 (41.0)	285.8 (18.6)	287.2 (11.4)	-	-	-	-
400 °C	283.9 (27.1)	284.9 (32.9)	286.0 (17.9)	287.2 (8.5)	288.6 (5.1)	290.1 (3.3)	291.4 (3.7)	293.1 (1.5)
600 °C	284.1 (33.3)	285.1 (33.4)	286.1 (16.7)	287.4 (7.0)	288.8 (4.5)	290.3 (3.5)	291.9 (1.6)	-
800 °C	-	284.8 (56.3)	286.1 (21.9)	287.5 (8.6)	289.0 (6.2)	290.5 (4.7)	292.2 (2.3)	-
1000 °C	-	284.8 (61.3)	286.2 (17.2)	287.6 (7.5)	289.1 (5.9)	290.6 (5.2)	292.2 (2.9)	-

carbons of PEI at 284.7 and 285.5 eV, respectively. Upon treatment at 200 °C, a new peak appears at lower binding energy, 283.8 eV, likely due to the aromatic carbon of functionalized C_{60}. The aliphatic and amine carbon of PEI are still present, but the relative concentration of C-C drops from 76 to 41% upon thermal decomposition of PEI. Furthermore, part of the amine functions is decomposed to amide functions corresponding to the peak at 287.2 eV. Oxygen signals were recorded in all XPS survey spectra of thermally treated PEI-C_{60}, as reported in Figure S2 of the Supporting Information, in agreement with the formation of amide (O=C-NH). The source of oxygen during thermal treatment in Ar flow is likely due to residual absorbed CO_2, which is known to act as a soft oxidizing agent.[24] Heating up to 600 °C caused a further oxidation of the sample with a range of new functional groups appearing with peaks at higher binding energy associated to the carbonyl groups of aldehydes, ketones, carboxylates, and possibly carbonates or π→π* shake-up satellites of aromatic structures.[25-27] Shake-up satellite

peaks correspond to the photoemission of C1s core electrons with lower kinetic energy (higher binding energy) due to the transfer of part of their energy to (and consequent 'shake-up' excitation of) the valence electrons of the aromatic moieties ($\pi \rightarrow \pi^*$ transitions).[28] After pyrolysis at 800 and 1000 °C the aromatic peak of C_{60} is not found – it is known[29] that the decomposition or transformation of C_{60} in inert atmosphere already begins when it is heated above 600 °C – whilst a main peak at 284.8 eV could be assigned to the presence of nested carbazole moieties or graphite-like sp^2 hybridized carbons.[30,31] The simultaneous presence of peaks at about 286 and 288 eV suggests that nitrogen could be incorporated in a graphite-like structure, similarly to what has been observed for N-doped graphene where peaks at similar binding energy were attributed to C-N bonds and oxygenated group structures.[31] In support to these assignments there is also a C/N atomic ratio (Figure 2c) of about 10 at 900 °C comparable to that of carbazole, $C_{12}H_9N$ – pyrrolic-N, and quinoline, C_9H_7N – pyridinic-N. Further evidence for the presence of such a type of structures is found in the N1s spectra, as discussed in the following paragraph. A schematic representation of the chemical moieties likely formed upon thermal treatment of PEI-C_{60} is given in Scheme 1.

The N1s spectrum of as prepared PEI-C_{60} is best fitted with two peaks at 398.2 and 399.0 eV corresponding to the different amine groups present in PEI (Figure 3). Branched PEI has primary, secondary and tertiary amine groups (roughly in the ratio of 1:1.2:0.76, respectively, as from supplier specification) that are subject to different chemical environments. The peak at 398.2 eV is likely related to more substituted amines, secondary and tertiary, while that at 399.0 eV to the primary amines. The rationale behind this assignment is that the peak position (chemical shift) is dependent on the electron density present on the nitrogen. Nitrogen bonded to more alkyl groups (i.e., secondary and tertiary amines) is subject to a positive inductive effect

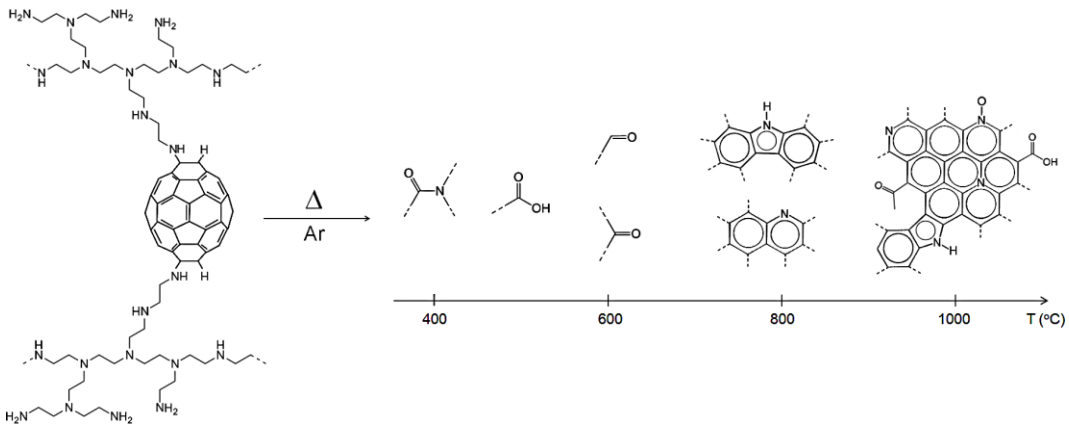

Scheme 1. Schematic representation of the chemical moieties formed upon thermal treatment of PEI-C_{60} in inert atmosphere. On the left, PEI-C_{60} showing a possible C_{60} linkage between two PEI molecules. On the right, some of the chemical moieties formed upon heating in Ar as identified with XPS: amide, carboxylic, aldehyde, ketone, carbazole, quinoline, and a nested combination of these chemical species.

that causes an increased electron density on the amine nitrogen. A higher electron density allows for a lower binding energy of the photoemitted electrons since it is easier to remove an electron from an electron enriched atom. This is a known effect, particularly in halogenated organic compounds where the strong inductive of effect of perfluorinated alkyl substitutes is responsible for large chemical shifts.[32]

A number of new peaks appear in the XPS N1s spectra of PEI-C_{60} upon thermal treatment (Figure 3). The peak positions, relative intensities, and suggested assignments are given in Table 2. Previous work by Kaptejin and co-workers[33] on the evolution of nitrogen functionalities in carbonaceous materials during pyrolysis helps in the assignment of the XPS peaks. Upon thermal treatment, the peaks of pyridinic-N and pyrrolic-N appear in the XPS spectra of pyrolyzed PEI-C_{60} at 398-399 eV and 400 eV, respectively. The latter one can also be related to pyridone

Table 2. XPS N1s peak positions (eV), relative intensities (%, reported in parenthesis), and assignments for as prepared and thermally treated PEI-C_{60}.

PEI-C_{60} Treatment T	Peaks and Assignments							
	Imine N	Amine / N-doped graphite / Pyridinic-N		Pyrrolic-N	Pyridinium-N	N-oxides of pyridinic-N / Nitro-N		
As prepared	-	398.2 (77.1)	399.0 (22.9)	-	-	-	-	-
200 °C	397.3 (11.2)	398.3 (35.9)	399.3 (43.4)	400.3 (9.5)	-	-	-	-
400 °C	-	397.8 (39.4)	398.9 (20.9)	399.9 (25.0)	400.8 (9.9)	402.5 (3.7)	-	404.6 (1.1)
600 °C	-	398.0 (42.3)	399.1 (15.4)	400.1 (23.2)	401.0 (10.8)	402.8 (5.3)	-	404.8 (3.0)
800 °C	-	398.4 (35.2)	-	399.9 (23.0)	401.0 (26.4)	402.3 (5.3)	403.3 (5.4)	404.9 (4.7)
1000 °C	-	398.4 (24.2)	-	399.8 (19.2)	401.0 (35.9)	402.3 (9.0)	403.3 (7.4)	404.9 (4.3)

moieties found at about 400.6 eV.[33] At higher binging energy, the peaks at 401 eV are associated to nitrogen atoms with a formal charge of +1 (quaternary nitrogen),[33] possibly in the form of pyridinium-N such as pyridinic-N protonated through the formation of a hydrogen bridge with a nearby hydroxyl or carboxyl group.[33] Moving further up, the peaks at 402-405 eV are tentatively associated to oxidized nitrogen.[33] Given these assignments, it is possible to evaluate the effect of pyrolysis on the nitrogen functionalities of PEI-C_{60}.

Heating PEI-C_{60} at 200 °C caused the conversion of part of the amine groups to pyridinic and pyrrolic nitrogen. The peak at lower binding energy, 397.3 eV, cannot be related to the presence of nitrile groups since their characteristic vibrational absorption bands are not observed in the IR spectra (*vide infra*). Tentatively, this peak could be associated to imine nitrogen atoms, as those present in emeraldine base polyaniline, for example.[28] A further increase of the pyrolysis temperature from 400 to 1000 °C takes the total amount of pyridinic-N + pyridinium-N to about

60%, that of pyrrolic-N to about 20%, and the remaining is oxidized N. This evolution is in agreement with what previously observed in the XPS C1s spectra. Upon thermal treatment in inert atmosphere, PEI-C_{60} is converted from a polymer composite characterized by many primary, secondary and tertiary amine functions to an N-doped graphite-like material where nitrogen is mainly integrated within 6-membered pyridinic rings, partially in 5-membered pyrrolic rings, or oxidized. In terms of CO_2 capture, these nitrogen and oxygen sites are directly involved in the physical interaction of CO_2 with pyrolyzed PEI-C_{60}. It is known that the presence of heteroatoms embedded or attached to graphitic layers can enhance CO_2 capture. This enhancement is associated with the electrostatic interactions between nucleophilic nitrogen and electrophilic CO_2.[34] In particular, N-doped graphitic carbons have the potential advantage to combine nucleophilic nitrogenated sites with surface defective regions where sp^3 hybridized carbon can affect the localization of electron density in sp^2 curved regions and facilitate CO_2 adsorption.[34,35]

The evolution of the chemical functionalities of PEI-C_{60} upon thermal treatment has been further investigated using ATR-FTIR, as presented in Figure 4. From the infrared spectra, it is once more evident that PEI-C_{60} undergoes major chemical changes with increasing pyrolysis temperature. The IR spectrum of as prepared PEI-C_{60} is characterized by two distinct sets of absorption bands. One set at 2500-3500 cm^{-1} is made of two contributions: (1) the C-H symmetric and asymmetric stretching of PEI (2500-3000 cm^{-1}), and (2) the N-H stretching of PEI possibly superimposed to the O-H stretching of adsorbed water (3000-3500 cm^{-1}). The other set of IR bands is at 1000-1800 cm^{-1} associated to the vibrational deformation of the methylenes of PEI (wagging at 1300 cm^{-1}, and scissoring at 1450 cm^{-1}), and to N-H and NH_2^+ deformation (1550-1650 cm^{-1}), and C-N stretching (1100 cm^{-1}).[36] These last features are referred as to the

"fingerprint" region of an infrared spectrum since it collects a populated series of vibrational absorptions specifically correlated to the chemical functionalities of a compound. Changes of peak intensities and positions in this region are expected when a material undergoes transformation, as observed in this case for PEI-C_{60}. Clearly, as the temperature of pyrolysis is increased, the fingerprint bands of PEI merge into a broader and featureless band that flattens almost completely at 800 °C. Nonetheless, the broad absorption feature observed in the range of

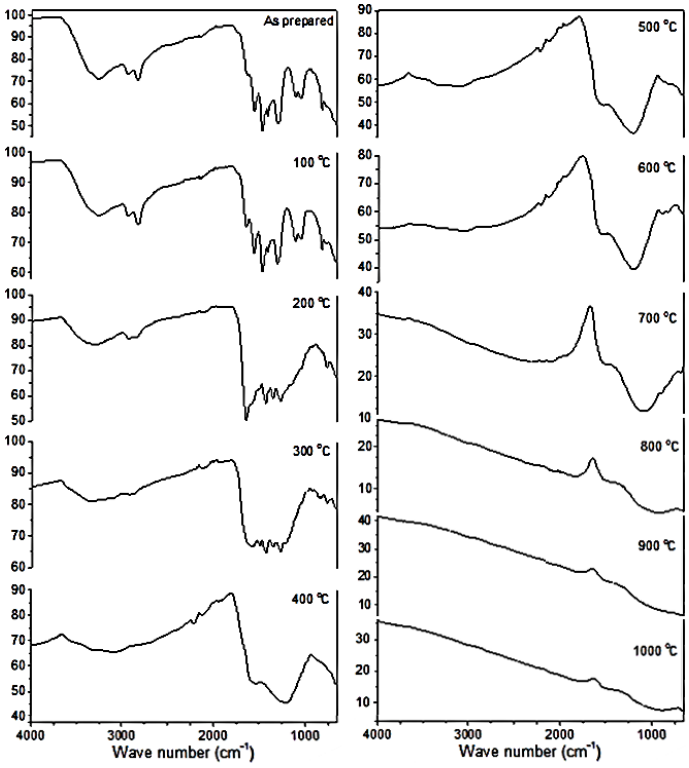

Figure 4. ATR-FTIR spectra of as prepared and thermally treated PEI-C_{60}. Treatment temperatures are given in each plot.

1600-1750 cm^{-1} for temperature of pyrolysis of up to 600 °C is likely related to the characteristic vibration of carbonyl containing functions such as those of carboxylic acid salts (1600 cm^{-1}) and pyridone (1650 cm^{-1}), for example.[36,37] A flattening of the 1000-1800 cm^{-1} region is similarly

observed for the C-H and N-H stretching bands at 2500-3500 cm^{-1}. Furthermore, the overall IR transmittance of the sample decreased with increasing temperature. PEI-C_{60} pyrolyzed at and above 800 °C strongly absorbs over all the spectrum range with value of infrared transmittance as low as 10%. Graphite materials are characterized by low transmittance, flat and featureless IR spectra.[38] This is in agreement with the XPS results discussed earlier, where it was found that N-doped graphitic materials are formed upon pyrolysis of PEI-C_{60} including pyrrolic-N and pyridinic-N.

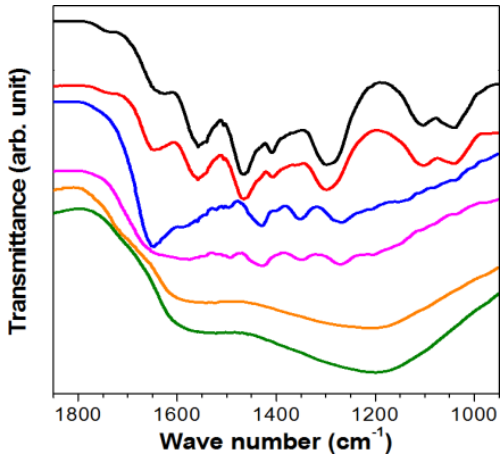

Figure 5. Fingerprint region of the ATR-FTIR spectra of as prepared and thermally treated PEI-C_{60}. Starting from the top: as prepared (black) PEI-C_{60}, and thermally treated, 100 °C (red), 200 °C (blue), 300 °C (magenta), 400 °C (orange), and 500 °C (green), PEI-C_{60}.

It is interesting to look at the progressive transition in chemical functionalities of PEI-C_{60} after thermal treatment in the lower temperature range, as from the fingerprint region of the infrared spectra of PEI-C_{60} shown in Figure 5. From an overall look at the spectra, heating above 400 °C causes a complete loss of features, as previously discussed. Otherwise, the treatment at

100 °C does not introduce any significant changes in the spectral features, meaning that the material is chemically stable at that temperature. Instead, already at 200 °C most of the absorption bands of PEI start fading, with in particular the band at 1100 cm^{-1} of C-N stretching entirely gone. At the same time, the intensity of the band of N-H deformation at 1650 cm^{-1} is strongly increased suggesting a breaking of the C-N bonds to form free amine groups, at the expense of the backbone integrity of PEI. The thermal braking of the C-N bonds of branched PEI has already been reported in the literature.[39] Products of thermal decomposition of PEI in inert atmosphere are ammonia, ethylamine, pyrrole and C-substituted ethylpyrroles. [38] C=C double bond formation has also been observed upon PEI thermal degradation (fracturing of C-N bonds with hydrogen transfer). [39]

These findings combined with a correspondent observed drop of CO_2 absorption performance of PEI-C_{60} after heating at 200 °C (Figure 1d), suggests that the breaking down of the PEI backbone is the cause of loss of performance. Heating at 200 °C in Ar, converts an as prepared spongy and dry-in-feel PEI-C_{60} into a sticky material that has very low CO_2 capture capacity at all investigated absorption temperatures. We propose that this change is due to the generation of amine groups upon breaking of the C-N bonds, the strong hydrogen bonding of these amines makes the material sticky and viscous causing a drop of CO_2 capture capacity. More amine groups do not always imply higher CO_2 capacity; pristine PEI serves as an example, also a sticky and viscous material where the strong hydrogen bonding between amine groups makes it a poor CO_2 absorbent.

The Raman spectra of PEI-C_{60} before and after pyrolysis are compared in Figure 6. As prepared PEI-C_{60} has two very broad and weak Raman bands that are difficult to correlate to any specific scattering process. No changes are observed upon heating at 200 °C. Instead, when the temperature is brought to 400 °C a peak appears and grows out of the background at 1600 cm^{-1} for pyrolysis at 600, 800 and 1000 °C. At these temperatures a second broader peak is also evident at 1300 cm^{-1}. These two peaks are the D (defective carbons) and G (graphitic basal plane

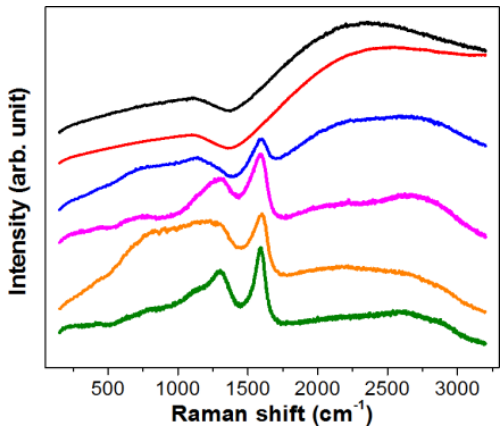

Figure 6. Raman spectra of as prepared and pyrolyzed PEI-C_{60}. Starting from the top: as prepared (black) PEI-C_{60}, and thermally treated, 200 °C (red), 400 °C (blue), 600 °C (magenta), 800 °C (orange), and 1000 °C (green), PEI-C_{60}.

carbon) bands typically found in this form and relative intensity for poly-crystalline and non-crystalline graphitic carbon.[40] Furthermore, graphitic materials usually have a G′ or 2D band at about 2600 cm^{-1} that in the present case may be either very broad or not present due to structural disorder or damaging of lattice.[41] Combing these findings with those previously discussed for the XPS and IR characterization, we can reasonably surmise that upon pyrolysis PEI-C_{60} is

converted from a cross-linked amine rich polymer composite to a disordered N-doped graphitic material characterized by the presence of pyrrolic, pyridinic , and oxidized nitrogens.

4. CONCLUSIONS

A detailed spectroscopy study of PEI-C_{60} thermally treated in argon over a wide range of temperatures reveals interesting aspects of how chemical changes and CO_2 sorption performance are correlated. The conversion of the amine functionalities of PEI-C_{60} to residual pyrrolic and pyridinic aromatic nitrogens upon pyrolysis is at the bases of the inversion of CO_2 capture behavior of pyrolyzed PEI-C_{60}. In particular, a unique transition temperature has been identified where an abrupt drop of CO_2 capture performance is observed. At 200 °C, the breaking down of the C-N backbone of PEI is responsible for this drastic deterioration in performance. This temperature works as a distinctive inversion point below and above which as prepared and pyrolyzed PEI-C_{60} can better capture CO_2 at high and low temperature, respectively. At the transition temperature, the depolymerization of PEI with limited loss of mass appears to free amino groups which in turn interact with each other through hydrogen bonding preventing them to be readily available for capturing CO_2.

AUTHOR INFORMATION

Corresponding Author

* E-mail: e.andreoli@swansea.ac.uk

ANKNOWLEDGMENTS

This work was supported by Apache Corporation, Inc., the Robert A. Welch Foundation (C-0002) and the Welsh Government Ser Cymru Programme. The authors declare no competing financial interests.

SUPPORTING INFORMATION AVAILABLE

Thermogravimetric profiles and XPS surveys of materials. This information is available free of charge via the Internet at http://pubs.acs.org/.

REFERENCES

(1) NOAA National Climatic Data Center, State of the Climate: Global Analysis for December 2014, published online, retrieved on June 14, 2015 from http://www.ncdc.noaa.gov/sotc/global/2014/12.

(2) Causes of Climate Change, published on line, retrieved on June 14, 2015 from http://www.epa.gov/climatechange/science/causes.html

(3) Pearce, D. The social cost of carbon and its policy implications. *Oxf. Rev. Econ. Policy* **2003**, *19*, 362-384.

(4) Moore, F. C.; Diaz D. B. Temperature impacts on economic growth warrant stringent mitigation policy. *Nature Clim. Change* **2015**, *5*, 127-131.

(5) Wang, J.; Huang, L.; Yang, R.; Zhang, Z.; Wu, J.; Gao, Y.; Wang, Q.; O'Hare, D.; Zhong, Z. Recent advances in solid sorbents for CO_2 capture and new development trends. *Energy Environ. Sci.* **2014**, *7*, 3478-3518.

(6) Chen, C.; Kim, J.; Ahn, W. S. CO_2 capture by amine-functionalized nanoporous materials: a review. *Korean J. Chem. Eng.* **2014**, *31*, 1919-1934.

(7) Dillon, E. P.; Crouse, C. A.; Barron, A. R. Synthesis, characterization, and carbon dioxide adsorption of covalently attached polyethyleneimine-functionalized single-wall carbon nanotubes. *ACS Nano*, **2008**, *2*, 156-164.

(8) Dillon, E. P.; Andreoli, E.; Cullum, L.; Barron, A. R. Polyethyleneimine functionalised nanocarbons for the efficient adsorption of carbon dioxide with a low temperature of regeneration. *J. Exp. Nanosci.* **2015**, 10, 746-768.

(9) Andreoli, E.; Dillon, E. P.; Cullum, L.; Alemany, L. B.; Barron, A. R. Cross-linking amine-rich compounds into high performing selective CO_2 absorbents. *Sci. Rep.* **2014**, *4*, 7304.

(10) Andreoli, E.; Cullum, L.; Barron, A. R. Carbon dioxide absorption by polyethylenimine-functionalized nanocarbons: a kinetic study. *Ind. Eng. Chem. Res.* **2015**, *54*, 878-889.

(11) Andreoli, E.; Barron, A. R. Effect of spray-drying and cryo-milling on the CO_2 absorption performance of C_{60} cross-linked polyethyleneimine. *J. Mat. Chem. A* **2015**, *3*, 4323-4329.

(12) Donahue, W. S.; Brandt, J. C. *Pyrolysis: Types, Processes, & Industrial Sources & Products*; Nova Science Publishers: Hauppauge, New York, 2009.

(13) Liu, C. J.; Wang, H. M.; Karim, A. M.; Sunand, J. M.; Wang, Y. Catalytic fast pyrolysis of lignocellulosic biomass. *Chem. Soc. Rev.* **2014**, *43*, 7594-7623.

(14) Morgan, T. J.; Kandiyoti, R. Pyrolysis of coals and biomass: analysis of thermal breakdown and its products. *Chem. Rev.* **2014**, *114*, 1547-1607.

(15) Uddin, M. N.; Daud, W. M. A. W.; Abbas, H. F. Effects of pyrolysis parameters on hydrogen formations from biomass: a review. *RSC Adv.* **2014**, *4*, 10467-10490.

(16) Lin, Z.; Waller, G.; Liu, Y.; Liu, M.; Wong, C. P. Facile synthesis of nitrogen-doped graphene via pyrolysis of graphene oxide and urea, and its electrocatalytic activity toward the oxygen-reduction reaction. *Adv. Energy Mat.* **2012**, *2*, 884-888.

(17) Debe, M. K. Electrocatalyst approaches and challenges for automotive fuel cells. *Nature* **2012**, *486*, 43-51.

(18) Xu, B.; Zheng, D.; Jia, M.; Cao, G.; Yang, Y. Nitrogen-doped porous carbon simply prepared by pyrolyzing a nitrogen-containing organic salt for supercapacitors. *Electrochim. Acta* **2013**, *98*, 176-182.

(19) Zhai, X.; Zhang, P.; Liu, C.; Bai, T.; Li, W.; Dai, L.; Liu, W. Highly luminescent carbon nanodots by microwave-assisted pyrolysis. *Chem. Commun.* **2012**, *48*, 7955-7957.

(20) Shinde, S. D.; Patil, G. E.; Kajale, D. D.; Gaikwad, V. B; Jain, G. H. Synthesis of ZnO nanorods by spray pyrolysis for H_2S gas sensor *J. Alloy Compd.* **2012**, *528*, 109-114.

(21) Zhao, C.; Kroll, A.; Zhao, H.; Zhang, Q.; Li, Y. Ultrasonic spray pyrolysis synthesis of Ag/TiO_2 nanocomposite photocatalysts for simultaneous H_2 production and CO_2 reduction. *Int. J. Hydrogen Ener.* **2012**, *37*, 9967-9976.

(22) Daranfed, W.; Aida, M. S.; Ataf, N.; Bougdira, J.; Rinnert, H. Cu_2ZnSnS_4 thin films deposition by ultrasonic spray pyrolysis. *J. Alloy Compd.* **2012**, *542*, 22-27.

(23) Nandi, M.; Okada, K.; Dutta, A.; Bhaumik, A.; Maruyama, J.; Derks, D.; Uyama, H. Unprecedented CO_2 uptake over highly porous N-doped activated carbon monoliths prepared by physical activation. *Chem. Commun.* **2012**, *48*, 10283-10285.

(24) Ansari, M. B; Park, S. E. Carbon dioxide utilization as a soft oxidant and promoter in catalysis. *Energy Environ. Sci.* **2012**, *5*, 9419-9437.

(25) Darmstadt, H.; Garcia-Perez, M.; Chaala, A.; Cao, N. Z.; Roy, C. Co-pyrolysis under vacuum of sugar cane bagasse and petroleum residue: properties of the char and activated char products. *Carbon* **2001**, *39*, 815-825.

(26) Payne, R. S. Parallel electron energy-loss spectroscopy and X-ray photoelectron spectroscopy of poly(ether ether ketone). *Polymer* **1993**, *34*, 1637-1643.

(27) Gardella, J. A.; Ferguson, S. A.; Chin, R. L. $\pi^* \leftarrow \pi$ shakeup satellites for the analysis of structure and bonding in aromatic polymers by x-ray photoelectron spectroscopy. *Appl. Spectrosc.* **1986**, *40*, 224-232.

(28) Yue, J.; Epstein, J. XPS study of self-doped conducting polyaniline and parent systems. *Macromolecules* **1991**, *24*, 4441-4445.

(29) Milliken, J.; Keller, T. M.; Baronavski, A. P.; McElvany, S. W.; Callahan, J. H.; Nelson, H. H. Thermal and oxidative analyses of buckminsterfullerene, C_{60}. *Chem. Mat.* **1991**, *3*, 386-387.

(30) Kessel, R.; Schultze, J. W. Surface analytical and photoelectrochemical investigations of conducting polymers. *Surf. Interface Anal.* **1990**, *16*, 401-406.

(31) Lv, R.; Li, Q.; Botello-Méndez, A. R.; Hayashi, T.; Wang, B.; Berkdemir, A.; Hao, Q.; Elías, A. L.; Cruz-Silva, R.; Gutiérrez, H. R.; Kim, Y. A.; Muramatsu, H.; Zhu, J.; Endo, M.; Terrones, H.; Charlier, J. C.; Pan, M.; Terrones, M. Nitrogen-doped graphene: beyond single substitution and enhanced molecular sensing. *Sci. Rep.* **2012**, *2*, 586.

(32) Carver, J. C.; Gray, R. C.; Hercules, D. M. Remote inductive effects evaluated by x-ray photoelectron spectroscopy (ESCA). *J. Am. Chem. Soc.* **1974**, *96*, 6851-6856.

(33) Pels, J. R.; Kapteijn, F.; Moulijn, J. A.; Zhu, Q.; Thomas, K. M. Evolution of nitrogen functionalities in carbonaceous materials during pyrolysis. *Carbon* **1995**, *33*, 1641-1653.

(34) Casco, M. E.; Morelos-Gómez, A.; Vega-Díaz, S. M.; Cruz-Silva, R.; Tristán-López, F.; Muramatsu, H.; Hayashi, T.; Martínez-Escandell, M.; Terrones, M.; Endo, M.; Rodríguez-Reinoso, F.; Silvestre-Albero, J. CO_2 adsorption on crystalline graphitic nanostructures. *J. CO_2 Utiliz.* **2014**, *5*, 60-65.

(35) Jiang, J.; Sandler, S. I. Separation of CO_2 and N_2 by adsorption in C_{168} schwarzite: a combination of quantum mechanics and molecular simulation study. *J. Am. Chem. Soc.* **2005**, *127*, 11989-11997.

(36) Socrates, G. *Infrared Characteristic Group Frequencies: Tables and Charts*; John Wiley & Sons: Chichester, England, 2004.

(37) Keller, G. L.; Bauer, L.; Bell, C. L. Infrared spectra of 2-pyridone-^{16}O and 2-pyridone-^{18}O. *Can. J. Chem.* **1968**, *46*, 2475-2479.

(38) Shulga, Y. M.; Baskakov, S. A.; Knerelman, E. I;. Davidova, G. I.; Badamshina, E. R.; Shulga, N. Y.; Skryleva, E. A.; Agapov, A. L.; Voylov, D. N.; Sokolov, A. P.; Martynenko, V. M. Carbon nanomaterial produced by microwave exfoliation of graphite oxide: new insights. *RSC Adv.* **2014**, *4*, 587-592.

(39) Nedel'ko, V. V.; Korsunskii, B. L.; Dubovitskii, F. I.; Gromova, G. L. The thermal degradation of branched polyethyleneimine. *Polymer Sci. USSR* **1975**, *17*, 1697-1703.

(40) Gonçalves, E. S.; Rezende, M. C.; Ferreira, N. G. Dynamics of defects and surface structure formation in reticulated vitreous carbon. *Brazilian J. Phys.* **2006**, *36*, 264-266.

(41) Xie, X.; Long, J.; Xu, J.; Chen, L.; Wang, Y.; Zhang, Z.; Wang, X. Nitrogen-doped graphene stabilized gold nanoparticles for aerobic selective oxidation of benzylic alcohols. *RSC Adv.* **2012**, *2*, 12438-12446.